ELSEVIER

Biophysical Chemistry 125 (2007) 237–246

Biophysical Chemistry

http://www.elsevier.com/locate/biophyschem

Photochemical probing of the B–A conformational transition in a linearized pUC19 DNA and its polylinker region

Karel Nejedlý *, Jana Chládková, Jaroslav Kypr

Institute of Biophysics, Academy of Sciences of the Czech Republic, Královopolská 135, CZ-612 65 Brno, Czech Republic

Received 3 May 2006; received in revised form 14 August 2006; accepted 16 August 2006
Available online 23 August 2006

Abstract

We induced the B-to-A conformational transition by ethanol in a linearized pUC19 DNA. A *primer extension* method was used in combination with UV light irradiation to follow the transition, based on pausing of DNA synthesis due to the presence of damaged bases in the template. *Primer extension* data highly correlated with the results of another method monitoring the B–A transition, i.e. inhibition of restriction endonuclease cleavage of UV light-irradiated DNA. *Primer extension* enabled us to locate damaged nucleotides within the region of interest. Most damaged nucleotides were located in B-form trimers, exclusively containing both pyrimidine bases (TTC, TCT, CTC, and CTT), and in a cytosine tetramer. The amount of damaged bases decreased in the course of B–A transition. Some of the damage even disappeared in the A-form, which mainly concerns the C_4 and C_3 blocks. The cleavage was nearly restored in the A-form within this region (*Eco*88I). On the contrary the decrease of damage was less significant with thymine dimers, only dropping to 50–60% of the B-form level. Consequently, the cleavage with *Eco*RI and *Hind*III remained mostly as before the transition (75% and 60% of uncleaved DNA preserved). We found significant differences in the B- and A-form pattern of UV light-damaged bases within the same region (polylinker) of DNA embedded within long (plasmid) or short (127 bp fragment) DNA molecules. The B–A transition of the fragment was found less cooperative than with linearized plasmid, which was confirmed by both CD spectroscopy and restriction cleavage inhibition.

Keywords: DNA; B–A transition; UV light; Primer extension; Restriction endonucleases; CD spectroscopy

1. Introduction

DNA can exist in two most common double helical architectures, the A-form and the B-form [1]. This was first observed in oriented fibers [2] and then in solution as well [3,4]. The B-form is adopted by DNA in dilute aqueous solutions or at high humidities in fibers whereas the A-form is stable at lower humidities in fibers or in the presence of ethanol and other substances in solution [5]. The B–A transition is highly cooperative [4] and the cooperativity originates from repuckering of the deoxyribose rings [6] and/or changes in hydration and ion binding [7].

The A-form of DNA is biologically very interesting because it is an almost constitutive conformation of double-stranded regions in RNA [8] and because it is induced in DNA by various polymerases [9–12], other proteins [13–16], polyamines [17,18], other cations [19] and ligands [20]. DNA can adopt an A-like double helix even when it contains sugars puckered in the B-like fashion [21,22]. Such a double helix is stabilized by $G_n{\cdot}C_n$ runs [21–26]. This unusual B/A hybrid is interesting from the evolutionary point of view because it suggests a possible way of transmission of molecular mechanisms developed on RNA to DNA during the RNA-to-DNA world transition [21,22]. In particular, this mainly concerns initiation of transcription and replication which are probably connected with the B–A transition of the transcribed or replicated DNA [13,27–30].

The B–A transition has been studied by a number of methods [2–4,31–34]. CD spectroscopy dominates among them because both the B-form and the A-form provide characteristic and substantially different CD spectra [3,4] and because CD samples can easily be titrated by ethanol or other agents inducing the B–A transition in DNA. However, CD spectroscopy and other biophysical methods mostly provide global pictures about the

* Corresponding author. Tel.: +421 541 517 202/189; fax: +421 541 211 293.
E-mail address: kane@ibp.cz (K. Nejedlý).

0301-4622/$ - see front matter © 2006 Elsevier B.V. All rights reserved.
doi:10.1016/j.bpc.2006.08.007

isomerizing DNA and they cannot be used to map B–A transition along genomic molecules of DNA. In addition, these methods cannot be used in complex biological contexts, e.g. in cell nuclei.

The only known method overcoming the limitation of the biophysical methods is the use of UV light to irradiate the isomerizing DNA and detection of the resulting damage. This approach was first used by Becker and Wang, who took advantage of the fact that the A-form is much more resistant to UV light damage than the B-form [33]. They detected the damage by chemical sequencing methods to probe the B–A transition of a part of the 5S ribosomal RNA gene. Recently we have extended this approach by using restriction endonucleases to detect the UV light damage of DNA in the B-form and A-form [35]. We have furthermore shown that the UV damage connected with its detection by restriction endonucleases can be used to detect B–A transition along the linearized pUC19 plasmid DNA [36]. Here we further extend our effort by the introduction of a *primer extension* detection of the damaged nucleotides in the isomerizing region of the pUC19 DNA. The present study reveals nucleotides or nucleotide regions which were most damaged due to UV light irradiation and reflected the changes in the course of B–A transition. A comparison with the restriction endonucleases cleavage pattern enabled us to correlate this macroscopic manifestation with the damage on the level of single bases. These results are promising for future studies where we will study the B–A transition induced by supercoiling in plasmid DNA, and in selected regions of the human genome.

2. Materials and methods

2.1. Materials

Plasmid pUC19 was bought from MBI Fermentas (Vilnius, Lithuania). Restriction endonucleases were purchased from MBI Fermentas, New England Biolabs (NEB; Beverly, MA, USA) and Promega (Madison, WI, USA). T4 polynucleotide kinase, the Klenow fragment and Phusion DNA polymerase were from NEB, Takara Bio Europe (Gennevilliers, France) and Finnzymes (Espoo, Finland), respectively. The commercial kits used were from Qiagen (MinElute PCR Purification Kit; Hilden, Germany), Princeton Separations (Centri.Spin-10; Adelphia, NJ, USA) and Amersham Life Sciences (Sequenase Version 2.0 DNA Sequencing Kit; Wien, Austria).

2.2. DNA sample preparation

The DNA samples used differed not only in their length (2686 and 127 bp) but also in the method of their production. Both of them had to be pure enough to be used for the B–A transition studies by CD spectroscopy or by UV light irradiation. The prerequisites were described previously [36].

2.2.1. Plasmid linearization

Plasmid pUC19 was linearized with an excess of *Ssp*I restriction endonuclease and purified by phenol and phenol/chloroform extraction to remove proteins.

2.2.2. Amplification of 127 bp long DNA fragment

Polymerase chain reaction (PCR) was performed with a linearized pUC19 plasmid as a template and 15- and 17-nucleotide long primers, selected in a way to have a polylinker about in the middle of the amplified fragment. High fidelity Phusion DNA polymerase (Finnzymes) ensured that a homogeneous fragment was obtained, which was purified with a MinElute PCR Purification Kit (Qiagen).

All DNA samples were ethanol precipitated, washed twice with 80% ethanol and dissolved in 1 mM EDTA (pH 7.2) as a stock solution. The homogeneity of the fragment DNA was verified by polyacrylamide electrophoresis, most of the fragment was sequenced as well (see further).

2.3. CD spectroscopy

CD spectra measurements in the course of conformational transitions of all DNAs were performed as described previously [36]. Briefly, the samples of DNA were complemented with ethanol to get a 62–63% concentration. Ethanol concentration was gradually increased by aliquot additions up to about 80%. After each addition, the CD value of ellipticity at 270 nm was taken. Usually after the finished B–A transition, 0.27 mM sodium phosphate buffer was added stepwise to follow the A–B transition, i.e. the reversibility of the B–A transition. DNA concentration was kept between 30 and 10 μg/ml in the course of the conformational transitions.

2.4. UV light irradiation

The conditions of irradiation were described in our previous paper [36]. DNA samples were irradiated at 5–12 μg/ml concentrations, in a final volume of 10 or 20 μl, respectively. The doses of UV light are indicated.

2.5. Restriction endonuclease cleavage

Irradiated DNA samples were dried out and dissolved in water. About 250 ng (plasmid) or 50 ng (fragment) of the DNA samples were complemented with the respective concentrated buffer and restriction endonuclease (10 units) in a final volume of 10 μl. After 2 h of cleavage at optimum temperature (37 °C) the digestion was terminated by addition of EDTA.

2.6. Electrophoresis and densitometry

DNA samples after restriction cleavage were electrophoresed in either 1.0% agarose (plasmid digestion), or 10% polyacrylamide gels (fragment digestion). Further processing and quantification were described elsewhere [35].

2.7. Primer extension

Primer extension was performed according to Sasse-Dwight and Gralla [37] with some modifications.

15 to 20 pmol of the primer were labeled in a final volume of 10 μl by 16 pmol of [γ-P^{32}]ATP and 5 units of T4 polynucleotide

kinase for 20 min at 37 °C. After addition of another 5 units of the enzyme, the incubation continued for another 20 min. The enzyme was thermally inactivated (65 °C, 20 min) and the labeled primer was devoid of unincorporated ATP and other small molecules by repeated centrifugal gel filtration (Centri. Spin-10; Princeton Separations) according to the manufacturer's instructions. The radioactivity of the lyophilized eluate was measured and set to $0.40–0.45 \times 10^6$ cpm/μl after dissolution.

Primer extension with the linearized plasmid followed the protocol referred to above [37]. Briefly, sodium hydroxide denatured template (about 0.14 pmol) and the primer (about 6×10^5 cpm) were neutralized, hybridized at 53 or 50 °C (upper and bottom strand primer, respectively) for 3 min, and cooled. After the addition of deoxynucleoside triphosphates and the Klenow fragment (1 unit), *primer extension* proceeded for 10 min at 50 °C. The EDTA terminated samples were precipitated, washed, and dried. The radioactivity of the samples was measured and dissolved to a concentration of 1×10^5 cpm/μl in a sequencing gel-loading solution.

Hybridization of a fragment (127 bp) with its primer was performed in a boiling water bath (2 min) followed by immediate cooling down on ice (to prevent hybridization of the complementary template strands). Further steps of the fragment *primer extension* were as above.

2.8. Sequencing electrophoresis and its quantification

The primer extension samples (1×10^5 cpm per slot) were separated on a denaturing sequencing gel (8% polyacrylamide containing 7 M urea) loaded on the gel next to the enzymatic sequencing reactions generated by *primer extension* of nonirradiated template DNA in the presence of the respective dideoxynucleoside triphosphate. Sequencing dideoxy reactions were performed according to the manufacturer's instructions (Amersham Life Sciences). Radioactive DNA fragments were observed by autoradiography at −70 °C with an intensifier screens and quantified by laser densitometry of autoradiograms [35]. Baselines were calculated from the graphs, peak integrals (baseline subtracted) were calculated and used for analysis. Because Klenow fragment terminated DNA synthesis just before the UV light-induced damage [38] while the terminating dideoxynucleoside triphosphates were incorporated, the latter migrated as if they were 1 bp longer.

3. Results and discussion

In our recent paper [36] we studied the B–A conformational transition in pUC19 plasmid by means of UV light irradiation followed by cleavage via a set of restriction endonucleases. We were able to detect the B–A transition with 16 tested restriction enzymes, because the A-form DNA was much more resistant to UV light damage than its B-form [33,35]. As the changes in cleavability with restriction endonucleases reflect UV light-induced damage within the whole recognition sequences (at least 6 bp) *plus* flanking nucleotides, we wanted to analyze the damage in more detail. The best resolution is at the level of single nucleotides, which allows comparing the site-localized manifestation of UV light induced damage in DNA (i.e. restriction cleavage inhibition) with its very basic cause, i.e. induction of covalent photoproducts. Another important point is that recognition sequences of restriction enzymes are not always available in the region of interest. The sequence fulfilling demands for an acceptable primer can be found much more easily.

For the single nucleotide resolution studies we utilized a method of *primer extension*, i.e. synthesis of a new DNA strand according to UV light-damaged DNA. In principle, the movement of DNA polymerase (Klenow fragment) along a template strand is halted by mono- or bifunctional photoproducts, which sterically prevent its further progress [39]. It does not matter of which nature the photoproduct is, either cyclobutane pyrimidine dimer or {6–4} photoproduct. In fact, it can also be a monofunctional photoproduct of an isolated pyrimidine base. We focused our attention mainly on the polylinker of pUC19 plasmid, because this 57 bp long DNA segment is a continual row of recognition sequences of ten restriction endonucleases and because it was exploited in our previous studies [35,36].

3.1. Conformational B–A transition of a linearized pUC19 plasmid

3.1.1. Primer extension of the UV light-irradiated plasmid DNA

Fig. 1 shows a typical sequencing gel of a pUC19 upper strand *primer extension*; the 57 bp long polylinker is indicated with a thick line. All the bands within the sample lanes are termination fragments, detecting the presence of photoproducts at the respective positions in the template (i.e. bottom) strand. The positions of damaged bases were identified, and the intensity of the respective termination fragments was quantified.

We performed an analysis of the occurrence and intensity of termination fragments in the B-form DNA in dependence on UV light dose in a range of 0.3–19.0 kJ m^{-2} (not shown). We noticed that, except for low doses (up to 1.0 kJ m^{-2}), there were relatively few qualitative differences between the various doses. The main difference was the quantitative one, the amount of termination fragments steeply increasing up to about 7.5 kJ m^{-2}. Further increasing of the doses slowed down the increase of intensity of the fragments, suggesting that it would reach a plateau. In contrast to the experiments with restriction enzyme cleavage, it was necessary to use lower doses of UV light irradiation to secure reasonable levels of termination fragments within the whole length of the polylinker. That is why we usually applied UV light doses of 2.5 and 5.0 kJ m^{-2} in our experiments.

Fig. 1 documents that the samples irradiated in both 80% and 85% ethanol differed significantly in the amount of termination fragments from the samples irradiated at lower ethanol concentrations. This agreed with CD spectroscopy results, showing that DNA was in the A-form at both 80% and 85% and in the B-form at 65% and lower ethanol concentration [36]. Fig. 2 summarizes the locations and semiquantitative representation of UV light-induced termination fragments within both strands of the pUC19 polylinker, in both B- and A-form of DNA. We found most B-form damaged bases within 5′-T*TC*-3′, 5′-T*C*T-3′, and 5′-CT*C*-3′ trimers in the upper strand and 3′-*C*TT-5′, 3′-*CC*CC-5′, 3′-T*C*T-5′, 3′-*T*TC-5′, and 3′-*C*TC-5′ in the bottom

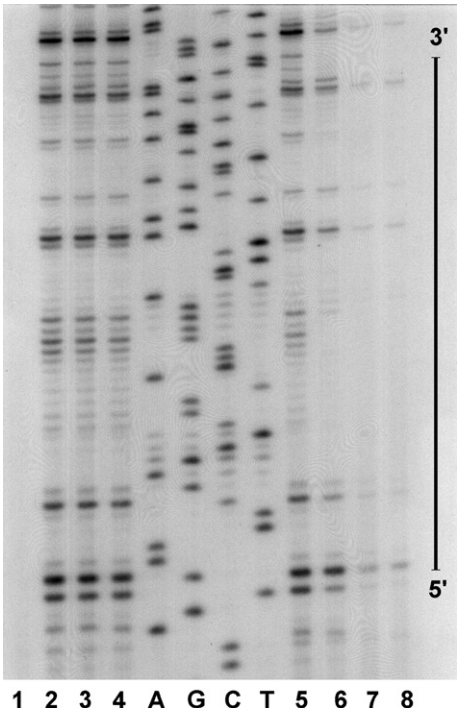

Fig. 1. *Primer extension* of a pUC19 plasmid upper strand, in the course of B–A transition, probed by UV light irradiation (2.0 kJ m^{-2}). Samples of linearized plasmid (*Ssp*I) were irradiated in the presence of 50%, 60%, 65%, 70%, 75%, 80%, and 85% ethanol (lanes 2–8), respectively. An unirradiated sample (lane 1) was incubated with 50% ethanol. All samples were used as templates for *primer extension*; radioactively labeled (T4 polynucleotide kinase and [γ-P^{32}] ATP) 17-mer was used as a primer. The purified samples were lyophilized, diluted in a sequencing gel-loading solution, and resolved on a sequencing gel together with A, G, C, and T dideoxy sequencing reactions. The dried gel was subjected to autoradiography. The thick line indicates the 57 bp long polylinker.

one. The C_4 tract was hit by UV light at all four bases, though at two of them much less, while the 5′-TCCTCT-3′ segment was only damaged in its 3′-end two bases.

Nearly all termination fragments decreased in their amount after the B–A transition was completed. Some of them even disappeared, suggesting that the corresponding bases in the template strand were not damaged at all. This is best demonstrated with the C_4 block in the bottom strand and with the C_3 tract in the upper one (Fig. 2). A similar, though less intense, effect was detected with cytosine dimers in the bottom and upper strands. On the other hand, the termination fragments corresponding to thymine dimers fell to about 50–60% of the B-form only. This different pyrimidine homodimer sensitivity to UV light was probably behind the different response to the B–A transition of the restriction cleavage by *Eco*RI and *Hind*III in comparison to *Kpn*I and *Eco*88I. In other words, when in the A-form, the recognition sequences of the latter enzymes became resistant to UV light damage, while the former remained mostly sensitive. A similar behavior as with *Eco*RI and *Hind*III was observed with restriction endonuclease *Xmn*I [36], containing a thymine tetramer in its pUC19 recognition sequence.

The last interesting point was the only one new damaged base in the A-form, i.e. thymine adjoining the 5′-end of the cytosine tetramer.

3.1.2. The primer extension pattern in the course of plasmid B–A transition correlates with restriction endonuclease cleavage changes

The results of *primer extension* mentioned above (Fig. 2 plus results not shown) allowed us to align all polylinker enzymes according to the decreasing extent of damage of bases in the respective recognition sequences, after plasmid irradiation in the B-form: *Eco*RI > *Xba*I > *Sac*I > *Hind*III > *Eco*88I > *Bam*HI > *Kpn*I > *Pst*I > *Sal*I > *Pae*I. From the results in Table 1, summarizing the restriction cleavage parameters after UV irradiation, we could make a similar row of polylinker enzymes according to the decreasing portion of uncleaved DNA after irradiation of the plasmid in the B-form: *Eco*RI > *Xba*I > *Sac*I > *Hind*III > *Eco*88I > *Bam*HI > *Kpn*I > *Sal*I > *Pst*I > *Pae*I. Though the data used for the construction of the former row were semiquantitative only and we did not include the effect of the damaged flanking bases, both rows were nearly identical.

When we inspect Fig. 2 with respect to the occurrence and amount of termination fragments within the recognition sequences of the respective restriction enzymes after irradiation in the A-form, we can notice three recognition sequences that were not significantly hit at any nucleotide: *Eco*88I, *Pst*I, and *Pae*I. A comparison with the data in Table 1 shows that cleavage with *Eco*88I of the plasmid UV light-irradiated in the A-form was practically not inhibited; the other two enzymes resumed their cleavage to a very high extent: about 90% of the uncleaved portion of DNA irradiated in the B-form was cleaved after the transition. On the contrary, we can see two recognition sequences (*Eco*RI and *Hind*III) that were still significantly UV

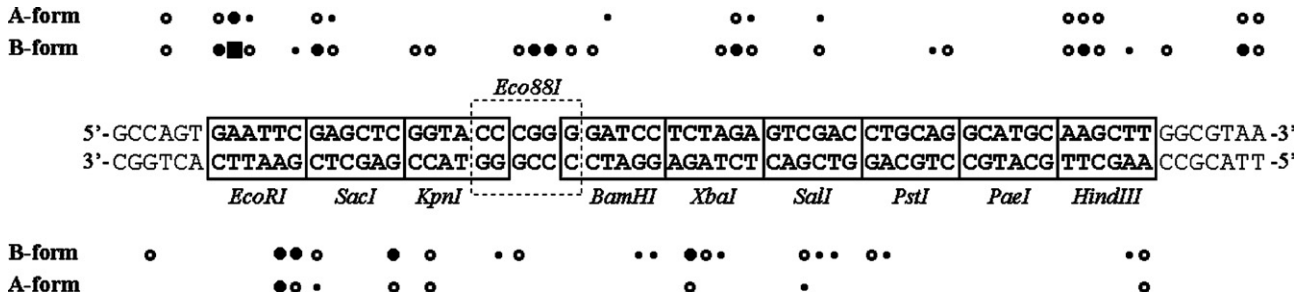

Fig. 2. The positions and semiquantitative representation of *primer extension* termination fragments induced by UV light irradiation (5.0 kJ m^{-2}) of the template pUC19 DNA both strands in the B-and A-form, respectively (50% and 80% ethanol). The positions of termination fragments are adjoined to the synthesized strands, i.e. the respective UV light damaged bases are in the complementary template strands. The amount of termination fragments in absorbance units is marked as: • (0.3–0.6), ○ (0.6–2.0), ●(2.0–6.0), and ■ (above 6.0). The recognition sequences of the restriction enzymes are marked off by the respective rectangles.

Table 1
Parameters of B- and A-form of linearized pUC19 plasmid as detected by restriction cleavage resistance upon UV irradiation

Restriction endonuclease	Uncleaved DNA[a]		Fraction of uncleaved DNA after B–A transition (%)[c]
	In B-form (%)[b]	In A-form (%)[b]	
*Eco*RI	33.4±2.9	25.0±3.0	74.8±9.0
*Sac*I	22.3±4.8	3.8±0.1	17.0±0.5
*Kpn*I	13.2±1.8	−1.0±0.9	−7.3±6.6
*Eco*88I	19.2±3.0	0.4±0.4	2.1±2.1
*Bam*HI	13.8±1.1	1.9±1.2	13.8±8.7
*Xba*I	25.9±0.8	4.7±0.6	18.1±2.3
*Sal*I	6.2±1.2	1.0±0.7	16.1±11.3
*Pst*I	4.5±1.7	0.5±1.8	11.1±40.0
*Pae*I	4.3±0.5	0.5±1.1	11.6±25.6
*Hind*III	22.0±0.1	12.9±2.1	58.6±9.5

[a] Average±SD of 3–5 independent experiments, each performed at ethanol concentrations ranging from 50% to 85%.
[b] 0% stands for cleavage of control, non-irradiated samples.
[c] Percentage of uncleaved DNA in A-form, in respect to amount of uncleaved DNA in B-form.

light-damaged in the A-form. As can be seen in Table 1, the majority of DNA not cleaved in the B-form was not cleaved in the A-form, either (75% and 59%, respectively). The recognition sequences of the five remaining enzymes preserved some UV light-induced damaged bases and their respective portion of uncleaved DNA in the A-form varied between 14% and 18% of the respective part in the B-form.

We further quantified the amount of the respective termination fragments in dependence on B–A transition. By way of illustration, we analyzed the results with *Eco*RI and *Xba*I (Fig. 3) — the enzymes that exerted a different sensitivity to UV light after B–A transition. With *Eco*RI, the majority of uncleaved DNA remained uncleaved after the transition (75% of the B-form level). Here we found five *primer extension* fragments, whose amount changed during the B–A transition. The strongest termination fragment had 62% of the B-form level (Fig. 3, left part, top strand) after the transition. The four weaker fragments (2/3–1/5 of the former) kept a smaller fraction of their B-form levels after the transition — 31%, 56%, 58%, and 57% (Fig. 3, left part), but their influence on the final macroscopic manifestation (i.e. *Eco*RI cleavage) was smaller (due to their lower proportion).

With the *Xba*I enzyme, the great majority of the DNA uncleaved after irradiation in the B-form became cleavable in the A-form (only 18% of the B-form level left uncleaved). The two strongest termination fragments within its recognition sequence (Fig. 3, right part) kept 23% and 35% of the B-form level, respectively, when irradiated in the A-form and mostly determined the final cleavage outcome. The three weaker fragments (1/2–1/5 of the former) kept 16%, 27%, and 44% of their counterparts in the B-form (%, right part) and had a moderate effect on *Xba*I cleavage.

The results with *Eco*88I showed a better correlation between the cleavage and amount of termination fragments within the B–A transition. All five fragments steeply disappeared due to the B–A transition (Fig. 2), which was accompanied by a nearly full (98%) recovery of the *Eco*88I restriction cleavage (Table 1).

These results proved a good correlation between the restriction cleavage of the respective sequence and the level of damage of the sensitive bases within the sequence, in the course of the UV light detected B–A transition. Besides, we could see a significantly higher resistance to UV light damage in the A-form of CC and TC blocks in comparison to thymine dimers.

We performed a similar quantification of termination fragments within the remaining recognition sequences. Most of them displayed a good correlation between the decrease of fraction of noncleaved DNA when UV-irradiated in the A-form (in comparison to the B-form) and the decrease of the amount of the most intensive termination fragments within the respective recognition sequences. The fraction of termination fragments within the recognition sequence of *Hind*III dropped to 43% (strong), 48%, and 60% (medium), respectively, of the B-form level; in comparison to the decrease of uncleaved DNA to 59%. Similarly with *Sac*I, two strong termination fragments fell to 22% and 18% of the B-form level, which well agreed with the 17% level of uncleaved DNA. An acceptable correlation was also attained with *Bam*HI (6.4% *versus* 14%) and *Pst*I recognition sequences (28% and 0% *versus* 11%). *Pae*I, which left only about 12% of uncleaved DNA in the A-form, did not show the presence of any termination fragment (in any noticeable amount) within its recognition sequence in either B- or A-form. Its uncleaved DNA portion was probably due to damage at the flanking sequences. A significant effect of flanking sequences should also be considered for the recognition sequence of SalI, when its decrease of the noncleaved DNA fraction (16% of the B-form level) was larger than the decrease of the amount of its termination fragments (to 37% and 38%). We should mention that with the enzymes that were less sensitive to UV light, we could expect a significant influence of the damaged flanking bases on the restriction cleavage inhibition. With all the three least UV light-sensitive enzymes (*Sal*I, *Pst*I, and *Pae*I) we should be aware that we are dealing with really small values. Consequently, these results were burdened with a greater uncertainty (see Table 1, SD in the third and fourth columns).

The most surprising results were obtained with the restriction sequence of *Kpn*I. Though its cleavability was entirely restored when irradiated in the A-form, the strongest termination fragment was preserved in as much as 54% of the B-form level. We analyzed the results of nine independent experiments and found that the termination fragment in question did not finish at the same position in the recognition sequence, but could be found at any one of the three adjoining nucleotides in different experiments. In the template strand, there was no pyrimidine dimer in the respective positions, whereas the presence of a pyrimidine dimer was an important condition for a UV light-induced photoproduct. We conclude that there was no photoproduct induced within the respective part of the recognition sequence. We suppose the effect of another anomaly, perhaps a bend that did not prevent restriction cleavage but was recognized by DNA polymerase.

3.2. B–A transition within the 127 bp long DNA fragment

The promising results with the pUC19 plasmid described above led us to the analysis of a shorter segment of DNA,

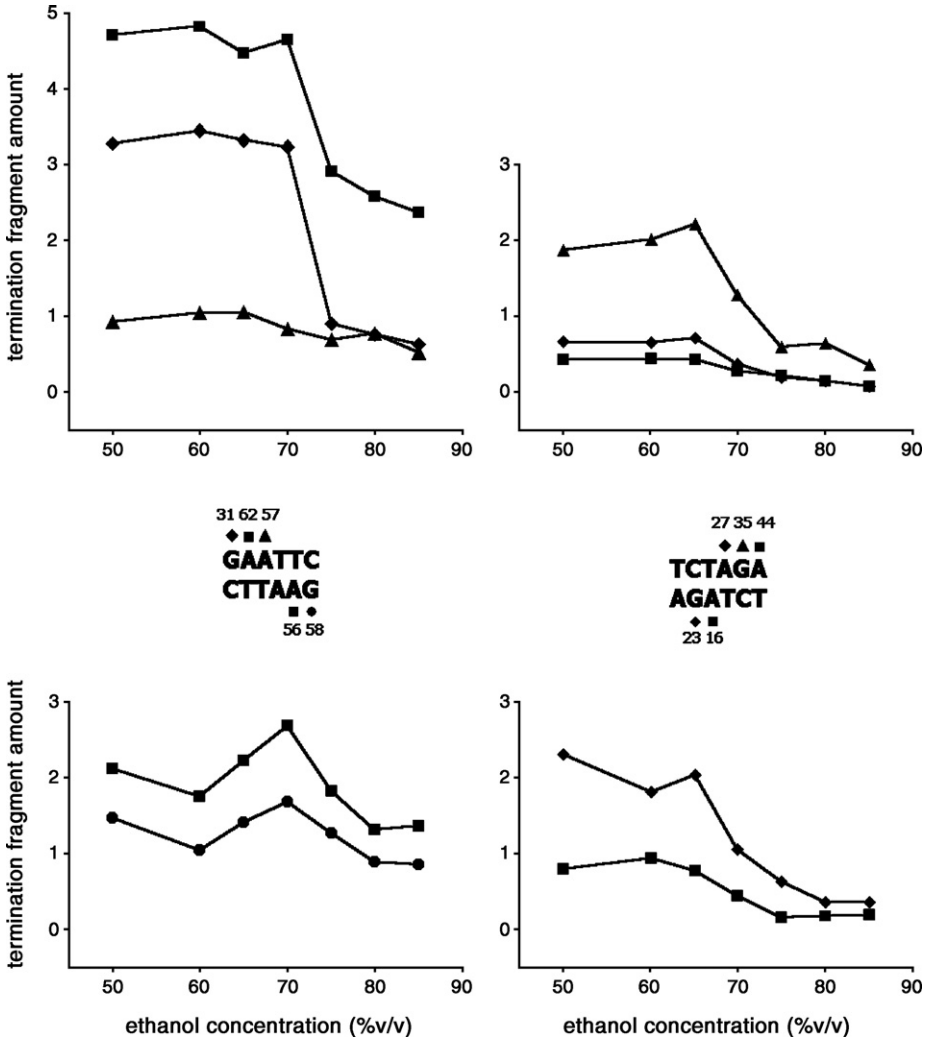

Fig. 3. Dependences of the amount of *primer extension* termination fragments induced by UV light irradiation (2.5 kJ m^{-2}) within the recognition sequences of *Eco*RI (left) and *Xba*I (right) in the course of B–A transition of linearized pUC19 plasmid (shown as ethanol concentration present when irradiated). The upper and bottom strand dependences are above and under the recognition sequences, respectively. These dependences are marked with the same symbols (closed circle, square, triangle, and diamond) as are the positions of the termination fragments within the *Eco*RI and *Xba*I recognition sequences, respectively. The numbers adjoining the respective nucleotides within recognition sequences denote fractions (%) of termination fragments after B–A transition, with respect to those in the B-form (average of four independent experiments). One of the experiments is shown, so the termination fragment intensity (in absorbance units) is mutually comparable within the figure.

composed mostly of recognition sequences of the previously studied restriction endonucleases (see above). We were interested whether it could be possible to detect any changes in the pattern of the B–A transition within a short fragment devoid of long flanking sequences. Nevertheless, the fact that in such a short molecule we could not analyze the whole polylinker via *primer extension* forced us to use a somewhat longer DNA molecule. Hence, we synthesized a 127 bp long PCR fragment whose polylinker core was flanked by 37 and 33 bp long segments, long enough for *primer extension* and subsequent sequencing gel analysis. This DNA underwent ethanol induced B–A transition as detected by CD spectroscopy, which was complete at about 76% of ethanol (Fig. 4). The midpoint of the transition was at about 73%, which agreed with the 72% obtained for seven fragments 80 to 301 bp long [40]. The transition was less cooperative in comparison to the transition of the pUC19 plasmid (Fig. 4), but it was significantly steeper (width about 6%) than with a shorter, 69 bp long fragment (Fig. 4).

3.2.1. Detection of B–A transition via UV light irradiation and restriction endonuclease cleavage of the fragment DNA

With a 127 bp long fragment we performed a similar analysis of B–A transition as we did with the linearized plasmid [36], i.e. DNA samples were UV light-irradiated at varying concentrations of ethanol and, consequently, they were digested by a set of 10 polylinker restriction endonucleases.

The dependences of the amount of restriction endonuclease resistant DNA on ethanol concentration generally showed abrupt decrease above 65% ethanol concentration (Fig. 5), corresponding to the B–A transition detected by CD spectroscopy (Fig. 4). These dependences looked similar to those obtained with the linearized plasmid [36]. In the fragment, this transition took a 5–10% ethanol concentration change for

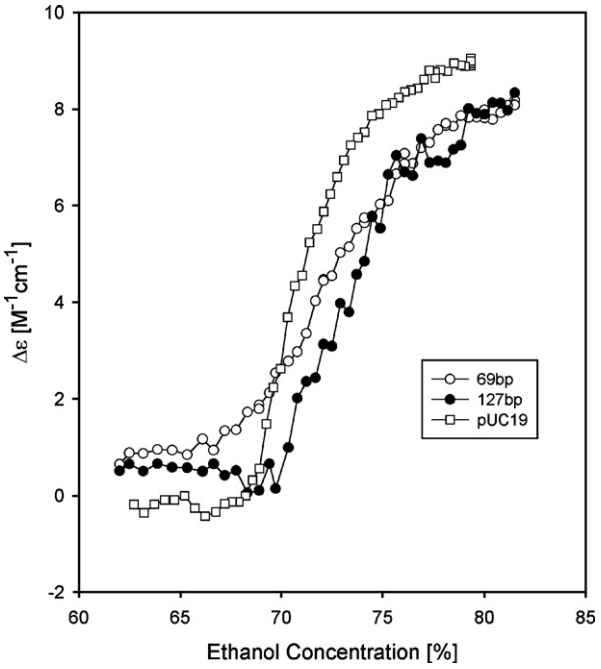

Fig. 4. CD spectroscopy of the B–A transitions of the DNAs analyzed in this study. Ethanol concentration dependences of the ellipticity at 270 nm with: 69 bp long synthetic fragment (open circles); PCR amplified, 127 bp long fragment (closed circles); and *Ssp*I-linearized pUC19 DNA (2686 bp; open squares).

*Bam*HI and about a 10% change for the majority of other enzymes (*Eco*RI, *Sac*I, *Eco*88I, *Xba*I, *Hind*III, SalI, *Pst*I). With *Kpn*I, it even reached about a 15% ethanol concentration change (Fig. 5).

Besides, there were significant quantitative differences with some restriction enzyme cleavage patterns. We found them when comparing the data in Table 2 (fragment) and Table 1 (plasmid). First of all, it concerned both terminal polylinker restriction endonucleases (*Eco*RI and *Hind*III), whose fractions of noncleaved DNA did not decrease much after the B–A transition in the plasmid: the fraction of uncleaved DNA only dropped to 75% and 59% of the values in the B-form, respectively (Table 1). This decrease became significantly larger with the fragment (Table 2): it dropped to about 50% (*Eco*RI) and 28% (*Hind*III), respectively. Similarly a significant decrease in the fraction of uncleaved DNA in the A-form fragment was found with two other restriction enzymes (compare Tables 2 and 1): 8% against 17% (*Sac*I) and 6% against 18% (*Xba*I). The *Kpn*I and *Eco*88I uncleaved DNA fractions fell to zero as it was observed with pUC19 DNA, while the four remaining enzymes showed a similar considerable decrease below 20% of the uncleaved DNA fraction in the A-form as observed with the plasmid.

3.2.2. Comparison of the changes in restriction endonucleases cleavage and primer extension of UV light-irradiated fragment due to B–A structural transition

Primer extension of the 127 bp fragment enabled us to study single nucleotide damage standing behind the changes detected by restriction endonuclease cleavage. The data summarized in Table 2 allowed us to align polylinker enzymes according to the decreasing portion of uncleaved DNA after UV light irradiation of the fragment in the B-form: *Eco*RI>*Xba*I>*Sac*I>*Eco*88I>*Hind*III>*Bam*HI>*Kpn*I>*Pae*I>*Sal*I>*Pst*I. This row slightly differs from that constructed for the plasmid (see the previous part) in only two mutual exchanges: *Eco*88I *versus Hind*III, and *Pae*I *versus Pst*I. The correlation of the row assembled according to the decreasing extent of damage of the bases within the recognition sequences after UV irradiation of the fragment in the B-form (*primer extension*; Fig. 6): *Eco*RI>*Xba*I>*Sac*I>*Bam*HI>*Hind*III>*Eco*88I>*Sal*I>*Kpn*I>*Pst*I>*Pae*I with that

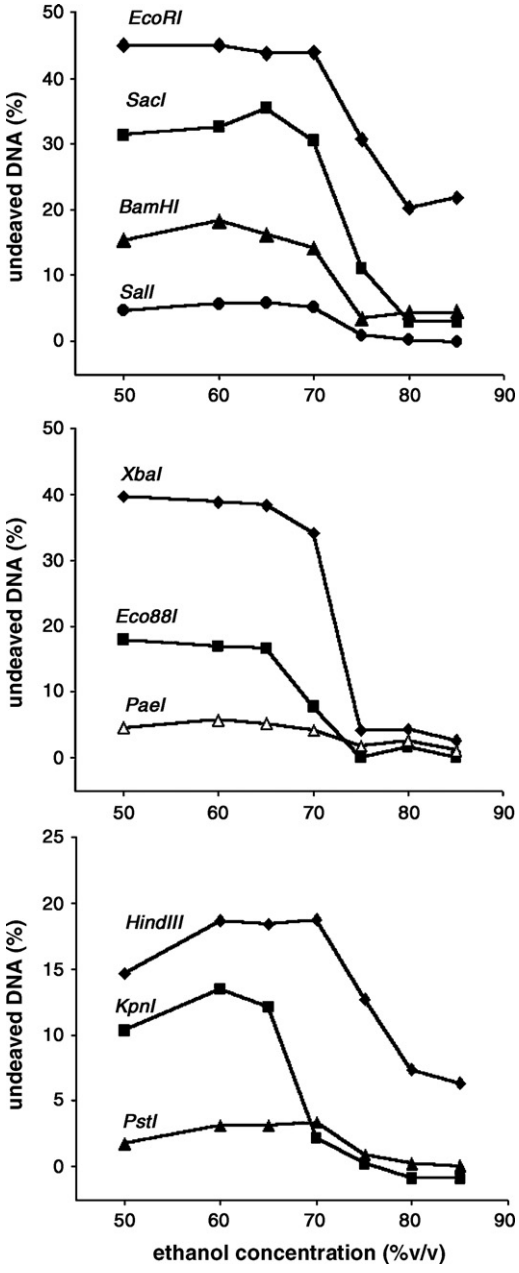

Fig. 5. Dependences of the amount of UV-irradiated DNA fragment, resistant to the indicated restriction endonuclease cleavage (%), on the concentration of ethanol present when the DNA was irradiated. The 127 bp fragment DNA samples were irradiated (concentration of about 12 μg/ml) in the presence of 0.1 mM EDTA with a dose of 15 kJ m^{-2}.

Table 2
Parameters of B- and A-form of 127 bp fragment as detected by restriction cleavage resistance upon UV light irradiation

Restriction endonuclease	Uncleaved DNA[a]		Fraction of uncleaved DNA after B–A transition (%)[c]
	In B-form (%)[b]	In A-form (%)[b]	
Eco*RI*	45.4±1.7	22.8±2.3	50.2±3.7
*Sac*I	28.1±6.8	2.2±0.9	7.6±1.9
*Kpn*I	10.2±2.0	0.1±0.8	1.3±7.5
*Eco*88I	20.7±2.9	0.2±0.5	1.2±2.3
*Bam*HI	17.5±0.8	3.1±0.9	17.7±4.7
*Xba*I	34.6±4.1	2.2±0.3	6.2±0.6
*Sal*I	5.9±0.7	0.3±0.6	4.2±7.3
*Pst*I	3.6±1.1	0.6±0.1	20.3±6.4
*Pae*I	6.4±1.4	1.5±0.6	23.3±4.9
*Hind*III	19.8±1.0	5.6±1.6	28.3±9.1

[a] Average±SD of 3–6 independent experiments, each performed at ethanol concentrations ranging from 50% to 85%.
[b] 0% stands for cleavage of control, non-irradiated samples.
[c] Percentage of uncleaved DNA in A-form, in respect to amount of uncleaved DNA in B-form.

shown above is significantly worse. Only four enzymes kept the same position, the rest moving by one or two places.

We tried to correlate the results of *primer extension* (i.e. changes in the amount of termination fragments) through the B–A transition with the changes in the restriction cleavage of the respective recognition sequences. We evaluated several enzymes differing in the manifested changes of the cleavage pattern after UV light irradiation, due to B–A transition (Fig. 6 and not shown). When the fragment was irradiated in the A-form, the termination fragments within the recognition sequences of *Kpn*I and *Eco*88I ceased almost completely, which was accompanied with a resumed restriction cleavage (Fig. 6 and Table 2). On the other hand, *Eco*RI and *Hind*III cleavage of the fragment irradiated in the A-form left 50% and 28% fractions of noncleaved DNA in the B-form, respectively (Table 2). With *Eco*RI, there was a correlation with the amount of the termination fragments decrease within its recognition sequence, which was between 50% and 60% of the B-form level for the three strongest termination fragments (not shown). Similarly, with *Hind*III, the two strongest termination fragments within its recognition sequence dropped to 24% and 32% of the B-form equivalents, respectively. A fairly acceptable agreement was noticed with *Xba*I as well: the strongest termination fragment decreased in the A-form to about 15% of the B-form level, two of three medium fragments dropped to zero, the third to about 40% (not shown). This agreed quite well with the 6% fraction of uncleaved DNA (Table 2).

3.3. Differences between the B–A conformational transition of the polylinker embedded in long and short DNA molecules as disclosed by UV light probing

The results described above enabled us to compare the pattern of B–A transition explored within the same sequence (57 bp) in both long (linearized pUC19 plasmid; 2686 bp) and short (127 bp) molecules of DNA.

The substantially different length of the DNA molecules probably stood behind the significant difference in cooperativity of the B–A transition of the plasmid and the fragment, as detected by CD spectroscopy (see Fig. 4). Similarly, we detected a less steep B–A transition by the restriction cleavage of the irradiated fragment in comparison to the irradiated linearized plasmid. A careful comparison of Fig. 5 with Fig. 2 of Ref. [36] showed that the B–A transition, manifested by an abrupt change of the portion of uncleaved DNA, is significantly steeper with plasmid DNA than with the fragment. With a good majority of polylinker enzymes, the transition from the B-form level of noncleaved DNA to the A-form level was nearly finished within a 5% ethanol concentration change (*Eco*RI, *Sac*I, *Eco*88I, *Bam*HI, *Xba*I, *Hind*III, SalI) in the plasmid. A less cooperative transition was observed only with *Kpn*I, which needed a 10% ethanol concentration change [36]. On the contrary, in the fragment this transition took at least 10% change (*Eco*RI, *Sac*I, *Eco*88I, *Xba*I, *Hind*III, SalI, *Pst*I), 5–10% for *Bam*HI. With *Kpn*I, it was at least a 15% concentration change (Fig. 5). This agreed with the above-described CD spectroscopy observation that the B–A transition was more cooperative with the pUC19 plasmid. Nevertheless, these differences are due to the effect of the whole length and state nothing about possible site-specific differences between the molecules.

There were three regions of the polylinker, where we could notice significant differences between the long plasmid and the short fragment molecules. Besides the terminal recognition sequences of the polylinker (*Eco*RI and *Hind*III, see Part 3.2.), the second interesting region was the recognition sequence of

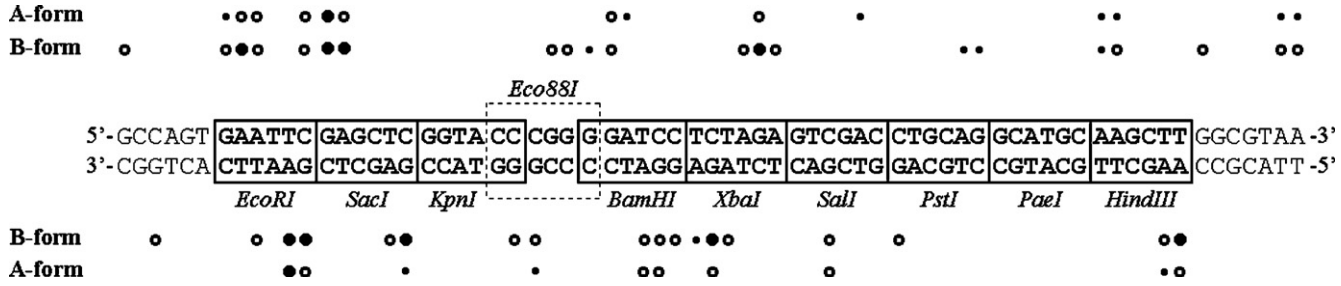

Fig. 6. The positions and semiquantitative representation of *primer extension* termination fragments induced by UV light irradiation (2.5 kJ m^{-2}) of the template 127 bp fragment DNA both strands in the B- and A-form, respectively (50% and 80% ethanol). The positions of termination fragments are adjoined to the synthesized strands, i.e. the respective UV light damaged bases are in the complementary template strands. The amount of termination fragments in absorbance units is marked as: • (0.2–0.6), ○ (0.6–2.0), and ● (2.0–6.0). The recognition sequences of restriction enzymes are marked off by the respective rectangles.

*Kpn*I restriction endonuclease. We found that the damage preserved in both B- and A-form of linearized plasmid DNA (perhaps a bend) did not appear in a short DNA fragment (Fig. 5). The third region was the cytosine tetramer that is part of the recognition sequences of both *Eco*88I and *Bam*HI. The 5′-terminal cytosine exhibited different behavior with plasmid and fragment DNA: in the plasmid it became resistant to UV irradiation in the A-form (as did the rest of the tetramer), while with the fragment DNA the level of damage even increased in comparison with the B-form (see Figs. 2 and 6). Contrary to the *Kpn*I region, we suppose that the damage is of a photoproduct nature, thus detecting a change in the structure of the fragment in the course of B–A transition.

Primer extension could hardly find any significant differences between the short and the long molecules of DNA irradiated in the B-form. More differences were found in the A-form. We could not compare the different sequencing experiments quantitatively (i.e., neither Fig. 2 nor 6), but we could relate the quantities of termination fragments in the B- and A-form DNAs in each experiment. Thus, the relative decrease in the intensity of termination fragments within the recognition sequence of *Eco*RI was about the same with both forms of DNA, while with *Hind*III it was significantly greater in the 127 bp fragment than in plasmid DNA. This explains the substantial drop of *Hind*III noncleaved DNA after irradiation in the A-form of the fragment in comparison to the plasmid.

What is the explanation of the differences between the long and short DNA molecules summarized above? It cannot be an effect of fragment ends — within the short molecule the region studied is more than 30 bp away from both ends. A possible explanation can be based on an idea of more or less stiff molecules depending on their length (for review see Ref. [41]). Our fragment molecule fits within the DNA persistence length, which is estimated to be around 250 bp, when both static and dynamic components are taken into account [42]. On the other hand, a linearized plasmid is long enough to be considered flexible and under constant thermal agitation. This difference in the rigidity of the molecules can be reflected in different sensitivity to UV light-induced damage. We believe that the significant differences on the level of *primer extension* termination fragments (e.g., recognition sequences of *Kpn*I, *Eco*RI, *Hind*III) could be explained in this way. Nevertheless, more experimental data is necessary to support this idea.

4. Conclusions

Conformational transitions of DNA have been studied for many years [43]. They include B–A and B–Z transitions, and transitions to less known non-B conformers of DNA. The non-B conformers frequently have different numbers of base pairs per repetitive double helix or other structural unit, which means that conformational transitions change DNA supercoiling. Thus, these transitions of DNA mostly involving tens of base pairs can be transmitted to a global scale of chromosome loops having about 50 kbp in length, whose supercoiling and the ensuing compaction can regulate the fundamental molecular biology phenomena [44–46].

The B–A, B–Z and other conformational transitions of DNA cannot be monitored by CD spectroscopy or other biophysical methods along pieces of genomic DNAs or in complex biological contexts, e.g. in cell nuclei. Success in these situations has partly been reported only with the use of UV light, which damages DNA, whereas the damage is sensitive to the physical state of DNA in the irradiated sample. The damage reflects contacts between the *lac* repressor and the operator in *E. coli* cells [47], regulatory protein–DNA interactions in mammalian genomic DNA [39], histone–DNA interaction [38], double-stranded and single-stranded states of the 5S rRNA gene [48], DNA arrangements into nucleosome cores [49], unusual conformation of $(dA)_n \cdot (dT)_n$ tracts in DNA [50], transcription factor binding to DNA [51], *Eco*RI endonuclease binding to DNA [52], and DNA triplex formation [53–56].

We think that the potential of the photochemical studies of DNA has not yet been exhausted by the above applications. We showed in our recent studies that restriction endonucleases can be used to detect conformation dependent UV damage in DNA [35] and that this approach can be used to map the B–A transition along linearized pUC19 DNA [36]. Here we extend our previous results with *primer extension* studies of the damage caused in DNA by UV light in the course of B–A transition. We were able to compare the B–A transition in the linearized pUC19 DNA and its fragment containing the polylinker region by three independent methods. The present and previous [36] work extend the spectrum of methods available to study the B–A transition along kilobase fragments of genomic DNA with the use of restriction enzymes as well as detection of the B–A transition at a single nucleotide resolution by the *primer extension* approach, both after UV light irradiation. We expect that the present results will be helpful in future studies of the ways in which the B–A transition is involved in transcription and replication.

Acknowledgements

This study was supported by grant A1004301 (K. N.) awarded by the Grant Agency of the Academy of Sciences of the Czech Republic, and by institutional grant AVOZ50040507.

References

[1] S. Arnott, D.W.L. Hukins, Optimised parameters for A-DNA and B-DNA, Biochem. Biophys. Res. Commun. 47 (1972) 1504–1509.
[2] R.E. Franklin, R.G. Gosling, The structure of sodium thymonucleate fibres. I. The influence of water content, Acta Crystallogr. 6 (1953) 673–677.
[3] J. Brahms, W.F.H.M. Mommaerts, A study of conformation of nucleic acids in solution by means of circular dichroism, J. Mol. Biol. 10 (1964) 73–88.
[4] V. Ivanov, L.E. Minchenkova, E.E. Minyat, M.D. Frank-Kamenetskii, A.K. Schyolkina, The B to A transition of DNA in solution, J. Mol. Biol. 87 (1974) 817–833.
[5] S.B. Zimmerman, B.H. Pheiffer, A direct demonstration that the ethanol-induced transition of DNA is between the A and B forms: an X-ray diffraction study, J. Mol. Biol. 135 (1979) 1023–1027.
[6] R. Soliva, F.J. Luque, C. Alhambra, M. Orozco, Role of sugar re-puckering in the transition of A and B forms of DNA in solution. A molecular dynamics study, J. Biomol. Struct. Dyn. 17 (1999) 89–99.
[7] A.K. Mazur, Titration in silico of reversible B–A transitions in DNA, J. Am. Chem. Soc. 125 (2003) 7849–7859.

[8] S. Arnott, W. Fuller, A. Hodgson, I. Prutton, Molecular conformations and structure transitions of RNA complementary helices and their possible biological significance, Nature 220 (1968) 561–564.
[9] W. Metzger, T. Hermann, O. Schatz, S.F.J. Le Grice, H. Heumann, Hydroxyl radical footprint analysis of human immunodeficiency virus reverse transcriptase–template primer complexes, Proc. Natl. Acad. Sci. U. S. A. 90 (1993) 5909–5913.
[10] A. Jacobo-Molina, J. Ding, R.G. Nanni, A.D. Clark, X. Lu, C. Tantillo, R.L. Williams, G. Kamer, A.L. Ferris, P. Clark, A. Hizi, S.H. Hughes, E. Arnold, Crystal structure of human immunodeficiency virus type 1 reverse transcriptase complexed with double-stranded DNA at 3.0 Å resolution shows bent DNA, Proc. Natl. Acad. Sci. U. S. A. 90 (1993) 6320–6324.
[11] S. Doublié, S. Tabor, A.M. Long, C.C. Richardson, T. Ellenberger, Crystal structure of a bacteriophage T7 DNA replication complex at 2.2 Å resolution, Nature 391 (1998) 251–258.
[12] J.R. Kiefer, C. Mao, J.C. Braman, L.S. Beese, Visualizing DNA replication in a catalytically active Bacillus DNA polymerase crystal, Nature 391 (1998) 304–307.
[13] V.L. Florentiev, V.I. Ivanov, RNA polymerase: two-step mechanism with overlapping steps, Nature 228 (1970) 519–525.
[14] S.C. Mohr, N.V.H.A. Sokolov, C. He, P. Setlow, Binding of small acid-soluble spore proteins from *Bacillus subtilis* changes the conformation of DNA from B to A, Proc. Natl. Acad. Sci. U. S. A. 88 (1991) 77–81.
[15] P. Setlow, DNA in dormant spores of Bacillus species is in an A-like conformation, Mol. Microbiol. 6 (1992) 563–567.
[16] V.I. Ivanov, L.E. Minchenkova, B.K. Chernov, P. McPhie, S. Ryu, S. Garges, A.M. Barber, V.B. Zhurkin, S. Adhya, CRP–DNA complexes: inducing the A-like form in the binding sites with an extended central spacer, J. Mol. Biol. 245 (1995) 228–240.
[17] E.E. Minyat, V.I. Ivanov, A.M. Kritzyn, L.E. Minchenkova, A.K. Schyolkina, Spermine and spermidine-induced B to A transition of DNA in solution, J. Mol. Biol. 128 (1978) 397–409.
[18] H. Robinson, A.H.-J. Wang, Neomycin, spermine, and hexaamminecobalt (III) share common structural motifs in converting B- to A-DNA, Nucleic Acids Res. 24 (1996) 676–682.
[19] C. Bauer, A.H.-J. Wang, Bridged cobalt amine complexes induce DNA conformational changes effectively, J. Inorg. Biochem. 68 (1997) 129–135.
[20] X.-J. Lu, Z. Shakked, W.K. Olson, A-form conformational motifs in ligand-bound DNA structures, J. Mol. Biol. 300 (2000) 819–840.
[21] L. Trantírek, R. Štefl, M. Vorlíčková, J. Koča, V. Sklenář, J. Kypr, An A-type double helix of DNA having B-type puckering of the deoxyribonuclease rings, J. Mol. Biol. 297 (2000) 907–922.
[22] R. Štefl, L. Trantírek, M. Vorlíčková, J. Koča, V. Sklenář, J. Kypr, A-like guanine–guanine stacking in the aqueous DNA duplex of d(GGGGCCCC), J. Mol. Biol. 307 (2001) 513–524.
[23] L.E. Minchenkova, A.K. Schyolkina, B.K. Chernov, V.I. Ivanov, CC/GG contacts facilitate the B to A transition of DNA in solution, J. Biomol. Struct. Dyn. 4 (1986) 463–476.
[24] T.E. Cheatham, J. Srinivasan, D.A. Case, P.A. Kollman, Molecular dynamics and continuum solvent studies of the stability of polyG–polyC and polyA–polyT DNA duplexes in solution, J. Biomol. Struct. Dyn. 16 (1998) 265–280.
[25] H.-L. Ng, M.L. Kopka, R.E. Dickerson, The structure of a stable intermediate in the A–B DNA helix transition, Proc. Natl. Acad. Sci. U. S. A. 97 (2000) 2035–2039.
[26] H.-L. Ng, R.E. Dickerson, Mediation of the A/B-DNA helix transition by G-tracts in the crystal structure of duplex CATGGGCCCATG, Nucleic Acids Res. 30 (2002) 4061–4067.
[27] R.S. Beabealashvily, V.I. Ivanov, L.E. Minchenkova, L.P. Savotchkina, RNA polymerase–DNA complexes. I. The study of the conformation of nucleic acids at the growing point of RNA in an RNA polymerase–DNA system, Biochim. Biophys. Acta 259 (1972) 35–40.
[28] W. Wachsman, D.D. Anthony, Conformational changes in deoxyribonucleic acid during transcription, Biochemistry 19 (1980) 5981–5986.
[29] W.A. Wlassoff, G.M. Dymshits, O.I. Lavrik, A model for DNA polymerase translocation: worm-like movement of DNA within the binding cleft, FEBS Lett. 390 (1996) 6–9.
[30] Y. Timsit, DNA structure and polymerase fidelity, J. Mol. Biol. 293 (1999) 835–853.
[31] T. Kursar, G. Holzwarth, Backbone conformational change in the A–B transition of deoxyribonucleic acid, Biochemistry 15 (1976) 3352–3357.
[32] J. Kypr, V. Sklenář, M. Vorlíčková, Phosphorus NMR spectra of natural DNA fragments in the course of the B-to-A conformational transition, Biopolymers 25 (1986) 1803–1812.
[33] M.M. Becker, Z. Wang, B–A transitions within a 5 S ribosomal RNA gene are highly sequence-specific, J. Biol. Chem. 264 (1989) 4163–4167.
[34] D.Y. Krylov, V.L. Makarov, V.I. Ivanov, The B–A transition in superhelical DNA, Nucleic Acids Res. 18 (1989) 759–761.
[35] E. Kejnovský, K. Nejedlý, J. Kypr, Factors influencing resistance of UV-irradiated DNA to the restriction endonuclease cleavage, Int. J. Biol. Macromol. 34 (2004) 213–222.
[36] K. Nejedlý, J. Chládková, M. Vorlíčková, I. Hrabcová, J. Kypr, Mapping the B–A conformational transition along plasmid DNA, Nucleic Acids Res. 33 (2005) e5.
[37] S. Sasse-Dwight, J.D. Gralla, Footprinting protein–DNA complexes in vivo, Methods Enzymol. 208 (1991) 146–168.
[38] Z. Wang, M.M. Becker, Selective visualization of gene structure with ultraviolet light, Proc. Natl. Acad. Sci. U. S. A. 85 (1988) 654–658.
[39] M.M. Becker, Z. Wang, G. Grossmann G, K.A. Becherer, Genomic footprinting in mammalian cells with ultraviolet light, Proc. Natl. Acad. Sci. U. S. A. 86 (1989) 5315–5319.
[40] W. Hillen, R.D. Wells, Circular dichroism studies of the B–A conformational transition in seven small DNA restriction fragments containing the *Escherichia coli* lactose control region, Nucleic Acids Res. 8 (1980) 5427–5444.
[41] W.K. Olson, V.B. Zhurkin, Twenty years of DNA bending, in: R.H. Sarma, M.H. Sarma (Eds.), Biological structure and dynamics, vol. 2, Adenine Press, Schenectady, 1996, pp. 341–370.
[42] J. Bednar, P. Furrer, V. Katritch, A.Z. Stasiak, J. Dubochet, A. Stasiak, Determination of DNA persistence length by cryo-electron microscopy. Separation of the static and dynamic contributions to the apparent persistence length of DNA, J. Mol. Biol. 254 (1995) 579–594.
[43] A. Bacolla, R.D. Wells, Non-B DNA conformations, genomic rearrangements, and human disease, J. Biol. Chem. 279 (2004) 47411–47414.
[44] A.-L. Paul, R.J. Ferl, Higher-order chromatin structure: looping long molecules, Plant Mol. Biol. 41 (1999) 713–720.
[45] D.A. Jackson, The principles of nuclear structure, Chromosom. Res. 11 (2003) 387–401.
[46] S. Semsey, K. Virnik, S. Adhya, A gamut of loops: meandering DNA, Trends Biochem. Sci. 30 (2005) 334–341.
[47] M.M. Becker, J.C. Wang, Use of light for footprinting DNA in vivo, Nature 309 (1984) 682–687.
[48] M.M. Becker, Z. Wang, Origin of ultraviolet damage in DNA, J. Mol. Biol. 10 (1989) 429–438.
[49] J.M. Gale, K.A. Nissen, M.J. Smerdon, UV-induced formation of pyrimidine dimers in nucleosome core DNA is strongly modulated with a period of 10.3 bases, Proc. Natl. Acad. Sci. U. S. A. 84 (1987) 6644–6648.
[50] V. Lyamichev, Unusual conformation of $(dA)_n \cdot (dT)_n$-tracts as revealed by cyclobutane thymine–thymine dimer formation, Nucleic Acids Res. 19 (1991) 4491–4496.
[51] S. Tommasi, P.M. Swiderski, Y. Tu, B.E. Kaplan, G.P. Pfeifer, Inhibition of transcription factor binding by ultraviolet-induced pyrimidine dimers, Biochemistry 35 (1996) 15693–15703.
[52] M.M. Becker, D. Lesser, M. Kurpiewski, A. Baranger, Jen-Jacobson, "Ultraviolet footprinting'' accurately maps sequence-specific contacts and DNA kinking in the *Eco*RI endonuclease DNA complex, Proc. Natl. Acad. Sci. U. S. A. 85 (1988) 6247–6251.
[53] V.I. Lyamichev, M.D. Frank-Kamenetskii, V.N. Soyfer, Protection against UV-induced pyrimidine dimerization in DNA by triplex formation, Nature 344 (1990) 568–570.
[54] V.I. Lyamichev, O.N. Voloshin, M.D. Frank-Kamenetskii, V.N. Soyfer, Photofootprinting of DNA triplexes, Nucleic Acids Res. 19 (1991) 1633–1638.
[55] M.S. Tang, H. Thun, Y. Cheng, J.E. Dahlberg, Suppression of cyclobutane and <6–4> dipyrimidines formation in triple-stranded H-DNA, Biochemistry 30 (1991) 7021–7026.
[56] V.A. Malkov, V.N. Soyfer, M.D. Frank-Kamenetskii, Effect of intermolecular triplex formation on the yield of cyclobutane photodimers in DNA, Nucleic Acids Res. 20 (1992) 4889–4895.